ASTRONOMY & ASTROPHYSICS
SUPPLEMENT SERIES

Astron. Astrophys. Suppl. Ser. **117,** 317-334 (1996)

uvby-β photometry of high-velocity and metal-poor stars. VIII. Stars of very low metal abundance⋆

W.J. Schuster[1,2], P.E. Nissen[3], L. Parrao[2], T.C. Beers[4] and L.P. Overgaard[3]

[1] Observatorio Astronómico Nacional, UNAM, Apartado Postal 877, C.P. 22800 Ensenada, B.C., México
[2] Instituto de Astronomía, UNAM, Apartado Postal 70–264, C.P. 04510, México, D.F., México
[3] Institute of Physics and Astronomy, University of Aarhus, DK–8000 Aarhus C, Denmark
[4] Department of Physics and Astronomy, Michigan State University, East Lansing, Michigan 48824, U.S.A.

Received September 7; accepted November 13, 1995

Abstract. — A catalogue of *uvby-β* photometry for 87 of the turn-off and subgiant stars from the HK survey of Beers et al. (1992) is given. Most of these stars have [Fe/H]≤ -2.5. These photometric data have been taken and reduced using the same techniques as in our previous two *uvby-β* catalogues. An error analysis has been made; typical mean observational errors for a star with $V = 14\overset{\mathrm{m}}{.}2$ are 0.008, 0.007, 0.011, 0.010 and 0.012 in V, $(b-y)$, m_1, c_1 and β, respectively. Our photometric data are also compared to the UBV photometry and spectral indices from the HK survey; satisfactory agreement is found indicating good quality for the two data sets. The stars are classified in reddening-free diagrams of the *uvby-β* system; several of the stars are found to have been mis-classified in the HK survey. Two metal-poor supergiants, three (possibly four) horizontal branch stars, one blue subluminous star and two stars with ambiguous photometry have been identified. Stellar parameters, such as $E(b-y)$, M_V, δM_V, and $T_{\rm eff}$, plus error estimates for these parameters, are provided using our photometric calibrations. Although all stars have galactic latitudes $|b| \geq 30^\circ$ many of them are significantly reddened with $E(b-y)$ ranging from 0.02 to 0.15. The average reddening towards the South Galactic Pole region, $b < -60^\circ$, is $E(b-y) = 0.027 \pm 0.004$ corresponding to $E(B-V) = 0.036 \pm 0.005$ in contrast to the low value of $E(B-V) \simeq 0.01$ derived from the Burstein & Heiles (1982) maps. The stars are analyzed in the $(b-y)_0$, [Fe/H] diagram, and individual ages estimated using the isochrones of VandenBerg & Bell (1985) and of Bergbusch & VandenBerg (1992). These very metal-poor stars are found to be coeval, within 1−2 Gyr, with the halo and thick-disk stars studied previously, with a mean age in excess of 18 Gyr. Several blue "thick-disk" stars, which are perhaps analogous to the "blue metal-poor" stars of Preston et al. (1994), have been identified.

Key words: stars: abundances — stars: distances — stars: fundamental parameters — dust, extinction — Galaxy: evolution — Galaxy: halo

1. Introduction

Galactic stars of extremely low metallicity provide crucial information for the investigation of the formation and evolution of the Galaxy, as well as on the nature of the early universe. These rare stars enable comparisons of the metallicity distribution function of very-metal-poor (hereafter VMP) stars with predictions of Galactic enrichment models (Beers 1987; Carney 1993), studies of the kinematics of metal-deficient stars as a function of abundance and distance from the Galactic plane (Allen et al. 1991; Majewski 1992; Beers & Sommer-Larsen 1995), and high-resolution observations which may be used to estimate the relative abundance of the light elements (Thorburn 1994; Boesgaard 1995) and heavy elements (Norris et al. 1993; McWilliam et al. 1995), which in turn place fundamental constraints on nucleosynthesis processes in the early universe. Of particular importance for studies of the light elements Li, Be, and B are the identification of VMP stars on or near the main sequence (hereafter MS), as problems associated with modeling the depletion of the light elements in the atmospheres of these stars during the course of subsequent evolution are avoided. There is also a clear advantage in identifying particularly bright MS VMP stars, so that high-resolution observations of the uniformly weak absorption lines of the light elements may be carried out with present-generation telescopes.

Send offprint requests to: W.J. Schuster, P.O. Box 439027, San Diego, CA, 92143-9027, U.S.A.

⋆Based on observations collected at the Danish 1.5 m telescope, La Silla, Chile, and at the Observatorio Astronómico Nacional at San Pedro Mártir, Baja California, México

Beers et al. (1985, hereafter BPSI) and Beers et al. (1992, BPSII) have listed numerous VMP stars which should prove suitable for carrying out the investigations discussed above. However, the photometric data for their low metallicity stars are limited, when it is available at all, to broadband UBV photometry. In particular for the BPSII stars without any published photometry, it is crucial to establish the proper classifications for the stars near the MS turnoff, where contamination of this sample from lower surface-gravity horizontal-branch stars and slightly-evolved subgiants is expected.

The *uvby-β* photometric system is particularly suited for the study of VMP F-type stars. Intrinsic color calibrations, $(b-y)_0$-β, allow accurate, $\pm 0\overset{\mathrm{m}}{.}01$, measures of interstellar reddening excesses, $E(b-y)$, for individual field stars; such a calibration has been given by Schuster & Nissen (1989a; hereafter Paper II). Evolutionary corrections of the form $\delta M_V = f\delta c_0$, from the c_0, $(b-y)_0$ diagram, allow us to derive accurate stellar distances even for evolving MS and subgiant stars; such calibrations and procedures have been discussed in Paper V (Nissen & Schuster 1991). Also, importantly, theoretical isochrones in the δM_V, $\log T_{\rm eff}$ diagram or transformed to the c_0, $(b-y)_0$ diagram allow the estimation of relative and absolute ages for evolving field stars which are near their respective turn-offs; in Papers III, V, and VII (Schuster & Nissen 1989b; Nissen & Schuster 1991; Marquez & Schuster 1994; respectively) the isochrones of VandenBerg & Bell (1985; VB85), of VandenBerg (1985; V85), and of Bergbusch & VandenBerg (1992; BV92) have been used to study the absolute and relative ages within the Galactic halo population and to make comparative analyses between the relative ages of the halo and thick-disk populations.

The *uvby-β* system also allows the measurement of stellar atmospheric parameters as a prelude to detailed abundance studies which will make use of high-resolution spectroscopy and model atmospheres. The reddening-corrected color $(b-y)_0$ can be transformed to $T_{\rm eff}$; empirical calibrations which include appropriate metallicity dependences have been given by Magain (1987) and by Olsen (1984). Also, the index diagrams, such as c_0, $(b-y)_0$ or the reddening-free $[c_1]$,β or $[c_1]$, $[m_1]$ diagrams, allow the classification of field stars according to their evolutionary status, such as MS star or subgiant; such techniques have been discussed and utilized by Strömgren (1966) and by Olsen (1984). The evolutionary status allows us to estimate the surface gravities of the field stars also for input into the model-atmosphere analyses.

In this Paper VIII, *uvby-β* photometry is given for 87 of the metal-poor stars from the survey work of BPSI and BPSII. Most of these stars have $V \lesssim 14\overset{\mathrm{m}}{.}8$, [Fe/H]$\leq -2.5$, and classifications of "TO" or "SG" (turn-off or subgiant stars). The observational errors are analyzed, and comparisons between these data and the photometric and spectroscopic data of BPSI and BPSII are made. These stars are studied and classified in the c_0, $(b-y)_0$; $[c_1]$,β; and $[c_1]$, $[m_1]$ diagrams, and stellar parameters such as $E(b-y)$, [Fe/H], distance, and $T_{\rm eff}$ are determined photometrically. These are compared with the corresponding parameters of BPSII. Relative ages are derived for these stars making use of the isochrones of VB85 and BV92, and the ages are compared to previous results for the high-velocity and metal-poor stars from the SN and SPC catalogues (Schuster & Nissen 1988; Schuster et al. 1993; respectively).

2. Photometric observations of the VMP stars

2.1. *Selection of the stars*

Most of the stars observed for this paper were selected from Table 5 of BPSII using the criterion $[\mathrm{Fe/H}]_{\rm c} \leq -2.5$, where $[\mathrm{Fe/H}]_{\rm c}$ is the corrected spectroscopic value derived by BPSII from the Ca II K line index using a calibration based on modern high-resolution spectroscopic [Fe/H] values. These non-kinematically selected stars have been identified using the techniques discussed in BPSI and BPSII.

To further restrict the sample to F-type stars, for which the *uvby-β* system was especially designed and for which relative ages might be obtained, the selected stars were restricted mainly to the bluer "TO" types (turn-off-star candidates) with a few "SG" types (subgiant candidates) added for comparison. For practical reasons, since the telescopes to be used were both of 1.5 m aperture, the magnitudes of the stars to be observed were limited to $V \lesssim 14\overset{\mathrm{m}}{.}8$. Most of the stars come from the SGP (South Galactic Pole) part of the survey as described in BPSI, but three were added from the NGP part without prior knowledge of their [Fe/H] or type. During the observations a few stars were emphasized for having possible unusual abundances, such as a Li depletion for 29527-015 (Thorburn & Beers 1993), or a CH-subgiant characteristic for 22898-027 (Thorburn & Beers 1992; McWilliam et al. 1995), or for a suspicion of being erroneously classified in BPSII, such as 22956-017 which is probably an sdB star.

One other star, 16927-017, is also a candidate metal-poor star from the northern objective-prism survey recently completed by Beers and collaborators. It was added to our list of objects when it was recognized to be a star with extremely low metal abundance, [Fe/H]≤ -3.0, based on a moderate-resolution spectrum obtained by R. Cayrel & T.C. Beers at the Observatoire Haute Provence, with broadband colors that place it near the MS turn-off, and with a rather bright apparent magnitude, $V = 11.7$.

2.2. *Observation and reduction techniques*

The *uvby-β* data presented here for the VMP stars were taken and reduced using very nearly the same techniques

as for the SN and SPC catalogues. All of the data were taken using 1.5 m telescopes: the Danish 1.5 m at the European Southern Observatory, La Silla, Chile (hereafter ESO), during observing runs in October 1992 and October 1993, and the H.L. Johnson 1.5 m telescope at the San Pedro Mártir Observatory, Baja California, México (hereafter SPM), during runs in November 1992, September 1993, and April 1994.

At both observatories the instrumentations were nearly identical six-channel *uvby-β* photometers, as the SPM one described in SN. The four-channel *uvby* sections are really spectrograph-photometers which employ exit slots and optical interference filters to define the bandpasses. At the beginnings of the five observing periods the grating angles of the spectrograph-photometers were adjusted using a cadmium lamp to position the spectra on the exit slots to within about ±1 Å. Whenever possible, extinction-star observations were made nightly over an air-mass interval of at least 0.8, and spaced throughout each night several "drift stars" were observed, first two hours east of the local meridian and then later two hours west of the meridian; with these observations the atmospheric extinction coefficients and time dependences of the night corrections could be obtained for each of the nights of observation (see Grønbech et al. 1976). Finding charts were employed at the telescope to identify all of the BPSII stars, and these charts were compared whenever possible to the original Schmidt plates used for detection of the metal-poor stars. For an unexplained reason the star 22960-029 has probably been mis-identified for this catalogue; the resulting *uvby-β* photometry is that of a mid-G, metal-rich dwarf star, in stark contrast to that expected for a VMP TO star. Program stars were integrated until at least 50,000 counts in all four channels of *uvby* and until at least 30,000 counts in both channels of Hβ. For the faint program stars, the sky was counted until its contributing error was equal to or less than the error of the stellar count.

As for the SN and SPC catalogues, all of the data reductions were done following the precepts of Grønbech et al. (1976) using computer programs kindly loaned to us by T. Andersen. The *uvby-β* standard stars observed were taken from the same lists as for the previous two catalogues; these are mostly secondary *uvby-β* standard stars from the catalogues of Olsen (1983, 1984). Also, a few of the more metal-poor stars from the SN catalogue were re-observed to check for consistency. The reduction programs create a single instrumental photometric system for the entire observing run, including nightly atmospheric extinction corrections and night corrections with linear time dependences. Then a single set of transformation equations to the standard systems of V, $(b-y)$, m_1, c_1, and β are obtained making use of all standard stars observed during that observing period. The equations for the transformation to the standard *uvby-β* system are the linear ones of Crawford & Barnes (1970) and of Crawford & Mander (1966). Second-order $(b-y)$ terms are included in the standard transformation equations for m_1 and c_1. Our y measures have been transformed to the V magnitude of Johnson et al. (1966). The average transformation coefficients for the *uvby-β* photometer on SPM from these data reductions are: $B = +0.039$, $D = 0.976$, $F = 1.083$, $J = +0.066$, $H = 1.012$, $I = +0.104$, and $L = 1.338$; these values are similar to the values found for the SN and SPC catalogues. The average transformation coefficients for the ESO photometer are: $B = +0.004$, $D = 1.003$, $F = 1.078$, $J = +0.007$, $H = 1.014$, $I = +0.034$, and $J = 1.179$. The transformation errors of these data reductions are similar to those of the SN and SPC catalogues: ±0.005 or better for $(b-y)$, and generally ±0.010 or better for V, m_1, c_1, and β.

2.3. *Accuracy of the uvby-β data*

An attempt was made to observe all of the faint VMP stars at least three times, combining the SPM observations with those of ESO; mainly stars north of declination −20° were observed at SPM. Many of the same standard stars were observed both at ESO and at SPM, the two photometers are nearly identical, and so no systematic differences should be expected between the data sets. Only two program stars, 22898-027 and 29527-015, were observed at both ESO and SPM, and their observations would indicate no systematic differences larger than $0\overset{\mathrm{m}}{.}013$. Of the 87 stars included in the present catalogue, 75 have 3 or more observations in *uvby* and 73 have 3 or more in Hβ. In Fig. 1 are shown the mean errors of V, $(b-y)$, m_1, c_1, and β as a function of V for those stars with 3 or more observations. These error plots have been fit with either first- or second-order polynomials as shown. These data are seen to be of high quality. The curves of Fig. 1 would indicate typical errors for V, $(b-y)$, m_1, c_1, β of about 0.010 mag at $V = 14\overset{\mathrm{m}}{.}2$. The average number of observations per star in Fig. 1 is about 3.4.

2.4. *The catalogue of uvby-β observations*

The *uvby-β* catalogue is given in Table 1 for the set of 87 metal-poor candidates observed at ESO and SPM. Column 1 of this table gives the stellar identifications according to the nomenclature of BPSI and BPSII. Column 2, the V magnitude on the standard Johnson UBV system. Columns 3-5, and 7, the indices $(b-y)$, m_1, c_1, and β, respectively, on the standard systems of Olsen (1983, 1984), which are essentially the systems of Crawford & Barnes (1970) and Crawford & Mander (1966) but with a careful extension to metal-poor stars and with north-south systematic errors corrected. Columns 6 and 8 give N_u and N_β, the total numbers of independent *uvby* and β observations, respectively.

Table 1. The standard *uvby-β* catalogue for the 87 BPSII stars

STAR	V	$b-y$	m_1	c_1	N_{uvby}	β	N_β	Note
16027-003	13.769	0.356	0.046	0.346	3	2.593	3	
16027-073	14.217	0.368	0.064	0.298	2	2.574	3	
16927-017	11.728	0.384	0.022	0.296	5	2.581	5	
16927-063	13.539	0.341	0.132	0.394	2	2.620	5	
22169-008	15.015	0.319	0.083	0.330	3	2.625	2	binary?
22171-037	14.933	0.317	0.025	0.408	3	2.568	3	horizontal branch?
22174-020	15.077	0.321	0.040	0.389	2	2.597	2	
22177-009	14.267	0.342	0.031	0.286	3	2.616	3	
22177-010	14.309	0.336	0.044	0.304	3	2.609	3	
22180-014	13.596	0.365	0.027	0.200	3	2.590	4	
22182-033	14.663	0.372	0.030	0.313	4	2.580	4	
22186-002	13.233	0.381	0.032	0.285	4	2.540	4	subgiant
22186-017	13.555	0.340	0.042	0.295	3	2.600	3	
22872-102	13.628	0.473	0.007	0.302	5	2.606	4	
22873-072	14.652	0.349	0.021	0.345	2	2.650	2	
22873-139	13.873	0.320	0.037	0.363	3	2.630	3	SB2 (Preston 1994)
22876-032	12.811	0.330	0.034	0.251	4	2.592	4	SB2 (Nissen 1989)
22877-013	14.646	0.403	0.075	0.120	3	2.535	3	binary?
22877-051	14.216	0.325	0.046	0.373	2	2.641	2	
22878-027	14.394	0.355	0.052	0.248	3	2.628	4	
22879-012	14.707	0.333	0.018	0.400	3	2.604	3	
22879-029	14.437	0.339	0.060	0.299	4	2.634	4	
22879-051	13.892	0.317	0.033	0.404	3	2.614	3	
22881-036	13.952	0.358	0.066	0.209	4	2.597	4	CH star
22881-070	14.400	0.316	0.036	0.398	4	2.634	4	
22884-033	14.538	0.406	0.029	0.350	2	2.635	3	
22884-108	14.265	0.396	0.036	0.351	4	2.638	4	
22888-014	14.423	0.321	0.045	0.294	3	2.619	3	
22888-031	14.907	0.353	0.023	0.213	3	2.597	3	
22890-011	14.701	0.314	0.055	0.409	3	2.618	3	
22892-025	14.018	0.322	0.047	0.336	3	2.644	2	
22893-005	14.221	0.435	0.012	0.268	3	2.564	3	
22893-015	14.806	0.367	0.036	0.321	4	2.589	4	
22893-030	14.215	0.384	0.021	0.310	3	2.590	3	
22894-019	13.935	0.361	0.028	0.246	3	2.608	3	
22894-049	14.380	0.373	0.041	0.202	2	2.583	2	offset in diaphragm
22898-027	12.871	0.373	0.083	0.279	5	2.594	5	CH star
22898-047	14.254	0.447	0.046	0.223	3	2.554	4	binary?
22942-024	14.159	0.311	0.062	0.365	3	2.638	4	
22943-095	11.762	0.324	0.045	0.335	3	2.619	3	
22943-132	13.361	0.357	0.034	0.223	4	2.570	4	
22944-014	14.192	0.346	0.044	0.288	4	2.559	4	
22944-061	14.307	0.406	−0.036	0.294	4	2.571	4	unusual?
22945-017	14.448	0.306	0.061	0.356	3	2.654	3	
22945-063	14.546	0.382	0.007	0.590	3	2.595	3	horizontal branch
22949-008	14.171	0.352	0.069	0.308	3	2.624	3	CH star
22949-030	13.885	0.338	0.034	0.301	3	2.599	3	
22952-011	13.764	0.346	0.023	0.378	3	2.601	3	
22953-037	13.621	0.323	0.024	0.371	4	2.623	4	
22954-004	14.267	0.345	0.009	0.368	4	2.593	4	
22955-054	14.848	0.041	0.054	0.327	2	2.659	2	sdB?, variable
22956-017	14.290	0.166	0.024	0.076	2	2.616	2	sdB
22957-019	13.717	0.341	0.025	0.331	3	2.622	3	
22957-024	14.307	0.324	0.037	0.361	3	2.617	3	

Table 1. continued

STAR	V	$b-y$	m_1	c_1	N_{uvby}	β	N_β	Note
22958-037	14.910	0.394	0.034	0.501	3	2.556	2	horizontal branch
22958-041	15.066	0.311	0.048	0.343	3	2.590	1	
22958-042	14.537	0.344	0.066	0.227	3	2.607	3	CH star
22958-052	14.224	0.315	0.047	0.366	5	2.618	4	
22958-065	14.485	0.344	0.038	0.296	3	2.576	3	
22958-074	14.802	0.362	0.027	0.248	3	2.629	3	
22960-029	13.469	0.550	0.453	0.268	2	2.551	1	metal-rich (misident.)
22963-004	14.988	0.453	−0.012	0.294	3	2.564	3	
22964-214	13.634	0.343	0.026	0.379	5	2.615	4	
22968-001	14.719	0.324	0.038	0.289	2	2.593	2	
22968-026	14.213	0.326	0.052	0.366	3	2.628	3	
22968-029	14.294	0.347	0.039	0.214	3	2.592	4	
29493-050	14.387	0.315	0.043	0.338	3	2.637	3	
29493-062	13.160	0.383	0.054	0.272	4	2.582	4	binary?
29493-094	14.097	0.313	0.041	0.369	3	2.612	3	
29499-003	14.313	0.318	0.046	0.382	3	2.605	2	
29499-060	13.050	0.305	0.052	0.357	4	2.609	3	
29501-051	14.006	0.429	0.024	0.462	3	2.571	2	horizontal branch
29504-006	14.474	0.293	0.053	0.346	3	2.609	3	
29506-007	14.195	0.326	0.038	0.399	3	2.629	3	
29506-090	14.349	0.328	0.034	0.361	3	2.626	3	
29512-013	14.007	0.303	0.024	0.860	4	2.665	3	supergiant, variable
29512-015	14.537	0.369	0.027	0.336	2	2.604	4	
29512-081	13.018	0.335	0.091	0.455	3	2.643	3	
29513-015	14.284	0.318	0.034	0.338	4	2.637	4	
29514-007	13.959	0.329	0.025	0.387	3	2.611	3	
29514-018	13.383	0.322	0.041	0.380	3	2.614	3	
29514-037	13.959	0.316	0.040	0.337	3	2.629	3	
29527-015	14.284	0.313	0.032	0.361	4	2.597	4	Li depleted
30312-062	13.010	0.370	0.006	0.830	3	2.644	3	supergiant
30339-069	14.739	0.312	0.032	0.397	3	2.628	3	
30339-080	14.732	0.329	0.031	0.309	3	2.606	3	
30493-071	13.255	0.336	0.054	0.346	3	2.591	3	

Column 9 of Table 1 gives notes for individual stars taken during the observations or during the data reductions and analyses. For example, 22894-049 was offset in the photometer diaphragm during the observations to exclude a fainter nearby star; since the bandpasses of the *uvby-β* photometers are mainly filter-defined, the small offset produces negligible errors for the indices. The star 22955-054 showed indications of photometric variability in $(b-y)$, m_1, c_1, and β, with mean errors 4.65, 4.4, 2.3, and 2.0 times those predicted by the mean curves of Fig. 1. Also, 29512-013 showed 18, 5, and 11 σ variations in V, $(b-y)$, and c_1. As will be shown below 22955-054 is probably an sdB star, and 29512-013 a metal-poor yellow supergiant. Finally, 22960-029 has the *uvby-β* photometry of a mid-G, metal-rich dwarf star rather than the VMP TO star that was intended; it has probably been misidentified. Other notes in Table 1 indicate possible composition anomalies or binary companions for the stars, based on the photometric indices and upon literature sources.

2.5. *Comparison with the BPSII photometry and spectral indices*

For more than half of the stars in Table 1, BPSII have obtained UBV photometry and for nearly all stars they have measured a spectroscopic index HP of the equivalent widths of the Hγ and Hδ Balmer lines. In order to check the quality of their data and of our *uvby-β* photometry, the agreement between the two sets of V magnitudes as well as the relations $(B-V)$ versus $(b-y)$ and HP versus β are examined.

Figure 2 shows V(BPSII) versus $V(uvby)$ for the 47 stars in Table 1 for which BPSII have obtained UBV photometry. The overall distribution of stars around the 1:1 line looks very satisfactory except for three stars which

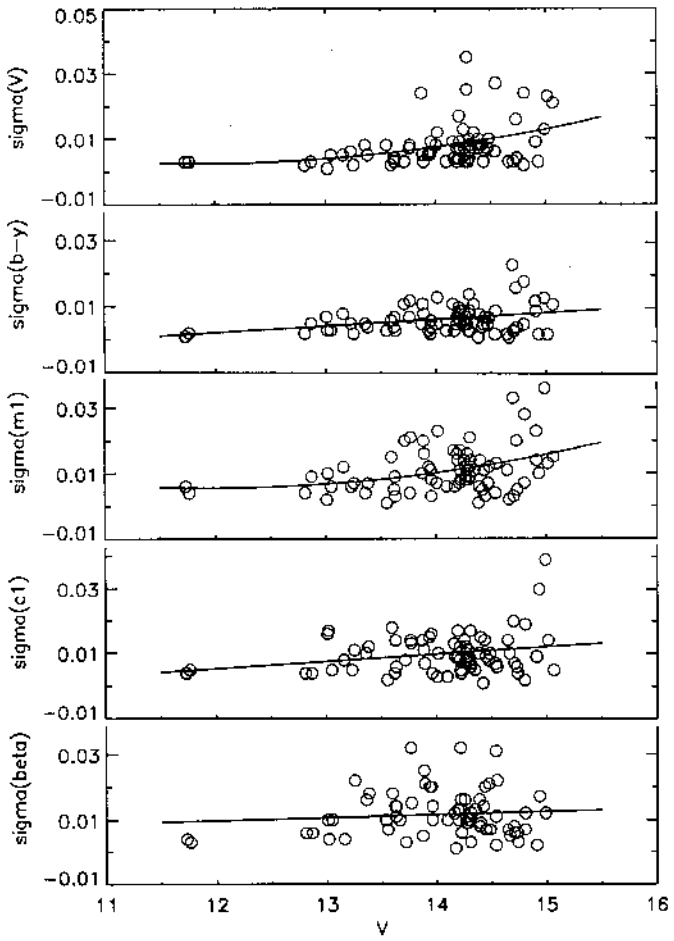

Fig. 1. Plots of the standard deviations of the mean for V, $(b-y)$, m_1, c_1, and β as a function of the visual magnitudes of the BPSII stars. Only stars with three or more observations have been plotted

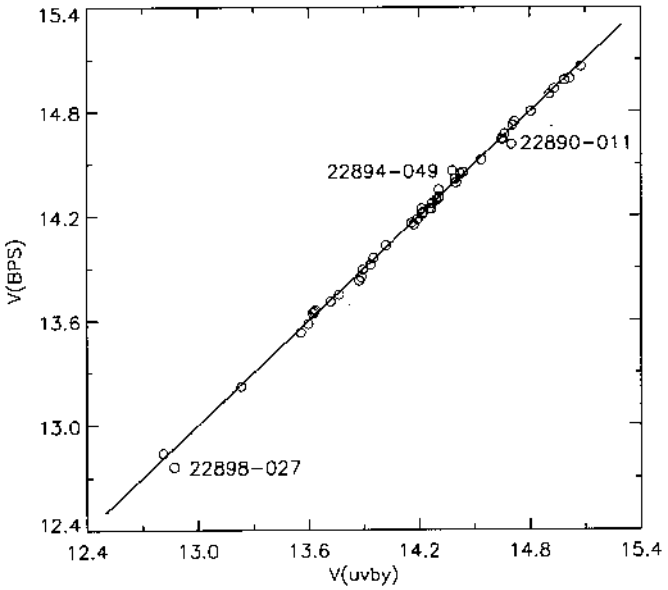

Fig. 2. V magnitudes from BPSII versus V magnitudes from the *uvby* photometry. The 1:1 line has been drawn, and three deviating stars with residuals $> 0\overset{m}{.}08$ marked

have residuals of the order of $0\overset{m}{.}08$ to $0\overset{m}{.}10$. One of these, 22894-049, is the star for which the photometry may be contaminated by a fainter star just outside the diaphragm. Another, the bright star 22898-027 deviates from the one-to-one line by six standard deviations; it would be interesting to check whether this star is a photometric and/or velocity variable, as the working model for the creation of essentially all CH subgiants invokes a binary mass-transfer scenario (McClure 1984; Vanture 1992). For the third star there is no obvious explanation for the deviation. Excluding these three outliers the average difference $\langle V(\mathrm{BPSII}) - V(uvby)\rangle$ is $-0\overset{m}{.}002$ and the rms deviation is $0\overset{m}{.}018$. This corresponds well to the combined errors in the photometry: $\pm 0\overset{m}{.}010$ in $V(uvby)$ and $\pm 0\overset{m}{.}015$ in V(BPSII) as estimated by Preston et al. (1991).

Figure 3 shows $(B-V)$ versus $(b-y)$. Three of the stars have anomalously high values of the G-band index and have been classified as CH stars by BPSII. These three all fall above the average relation between $(B-V)$ and $(b-y)$ having residuals of about $0\overset{m}{.}04$ in $(B-V)$. This seems reasonable since enhanced CN and CH absorption decreases the flux in the B band, whereas V, b, and y are not affected. Furthermore, the star 22944-061, which has been noted to have an unusually low m_1 index, has a large deviation from the mean relation. Excluding this star and the CH stars, a straight line has been fit to the data taking into account errors in both coordinates (see Press et al. 1992, p. 660). For $(b-y)$ the individual error estimates discussed earlier were used; a typical value is $\pm 0\overset{m}{.}007$. For $(B-V)$ an error of $\pm 0\overset{m}{.}009$ has been adopted, as given by Preston et al. (1991). The resulting line,

$$\begin{aligned}(B-V) &= 1.347(b-y) - 0.048 \\ &\quad \pm.035 \qquad \pm .012,\end{aligned} \tag{1}$$

is shown in Fig. 3. The reduced chi-square of the fit is $\chi^2/\nu = 1.56$ indicating that the errors in $(b-y)$ and/or $(B-V)$ may have been slightly underestimated.

Figure 4 shows HP versus β for the 77 stars in Table 1 that are included in BPSII. Since both indices measure the strengths of Balmer lines and are unaffected by interstellar reddening, a close relation would be expected. The scatter in Fig. 4 is, however, rather large. Adopting the errors in β discussed earlier (typically $\pm 0\overset{m}{.}012$) and the error of HP given by BPSII (± 0.1 Å), it is not possible to explain the scatter in Fig. 4. Increasing the error of HP to ± 0.2 Å, which seems more reasonable for the faint stars of Table 1, the following straight-line fit to the points is obtained,

$$\begin{aligned}\mathrm{HP} &= 21.58\beta - 53.12 \\ &\quad \pm 0.91 \quad \pm 2.37,\end{aligned} \tag{2}$$

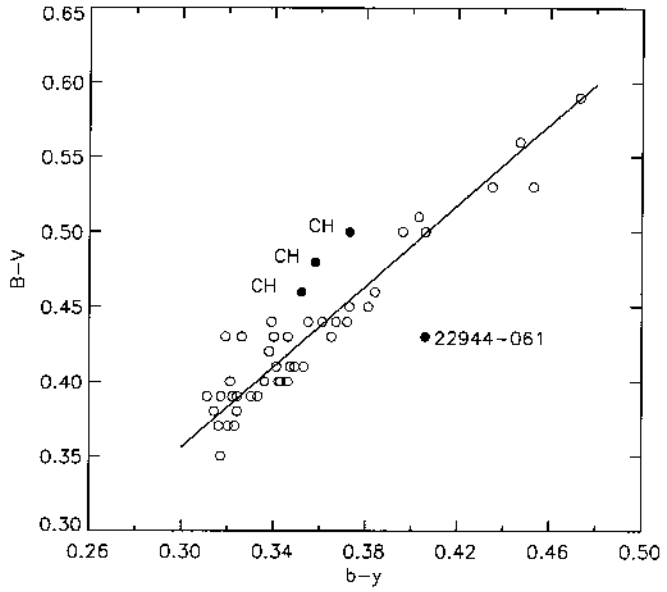

Fig. 3. $(B-V)$ versus $(b-y)$. CH stars and the peculiar star 22944-061 are marked. The straight-line fit to the open circles, with errors in both coordinates, is shown

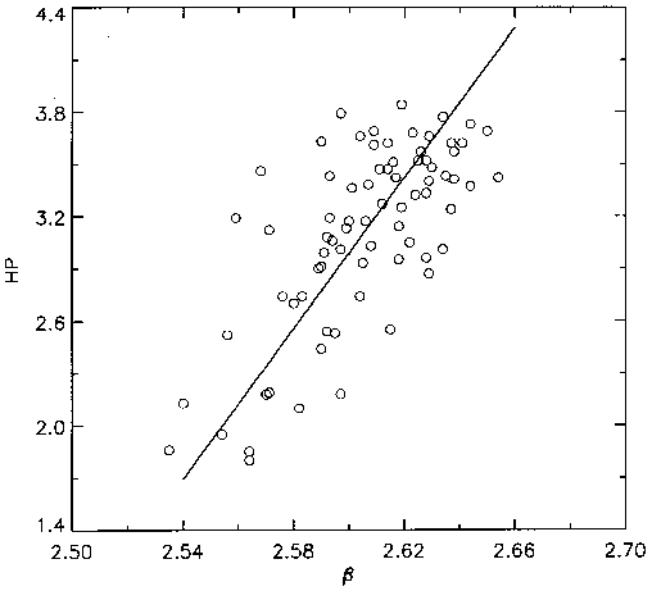

Fig. 4. The Balmer-line index HP versus β. The straight-line fit with errors in both coordinates is shown

with a reduced chi-square of $\chi^2/\nu = 1.6$, acceptable but also suggesting that the errors of β and/or HP are still higher than estimated. One effect that could contribute to an additional scatter of β are the shifts of the Hβ line due to large radial velocities, especially if the narrow β-filter is not well centered on Hβ (see the discussion in Paper II). Correlations between the residuals in the β-HP relation and the radial velocities of the stars have been checked, but none has been found. It is conceded that the original estimate of the error of HP ($\pm$0.1 Å) made by BPSII is probably too small for the faint stars of this paper; this estimate was made using some of the brighter stars first observed for the HK survey. σ(HP) = $\pm$0.2 Å is more realistic. Even then it is notable that the HP index gives as accurate a determination of $T_{\rm eff}$ as does the β index for the present data sample; $\sigma_{\rm HP} = 0.2$ Å implies $\sigma_\beta \cong 0\overset{\rm m}{.}01$ from the slope of Eq. (2).

3. Results

3.1. *Classification of the stars*

In Fig. 5 is given the reddening-free $[c_1]$, $[m_1]$ diagram, where $[c_1] = c_1 - 0.20(b-y)$ and $[m_1] = m_1 + 0.30(b-y)$ are the indices defined by Strömgren (1966), the only difference being that $E(m_1)/E(b-y) = -0.30$ has been used according to the work of Crawford (1975a). This diagram is given first since several of the BPSII stars fall outside the applicable range of the intrinsic-color calibration of Paper II. Only the 80 stars with corrected spectroscopic metallicities, $[{\rm Fe/H}]_{\rm c} \leq -2.5$ from BPSII, are plotted; the four NGP stars, one probably mis-identified star, and two stars from BPSII without $[{\rm Fe/H}]_{\rm c}$ values have been omitted. (Four of these omitted stars, 16027-003, 16027-073, 16927-017, and 29527-015, have [Fe/H]$\lesssim -1.50$ according to the photometric [Fe/H] calibration of Paper II; these four fall in the ranges, $0.126 \leq [m_1] \leq 0.174$ and $0.219 \leq [c_1] \leq 0.275$, similar to the majority of stars of Fig. 5).

In Fig. 5 most of the stars which were classified "TO" or "SG" by BPSII fall in a clump, within the limits $0.12 \lesssim [m_1] \lesssim 0.16$ and $0.12 \lesssim [c_1] \lesssim 0.35$, corresponding to the MS and turn-off (TO) stars of an extreme Population II. Due to the very low metallicity of the BPSII stars, our Fig. 5 is shifted by ≈ -0.10 in $[m_1]$ with respect to the same diagram of Strömgren (1966, Fig. 1). However, several stars are seen to lie outside this main clump of Fig. 5. In analogy with Fig. 1 of Strömgren (1966), it can be concluded that the stars of our Fig. 5 with the larger $[c_1]$ values, such as the five with $[c_1] \gtrsim 0.35$, are probably more highly evolved, such as horizontal branch, AGB, or metal-poor supergiant stars. The five stars with $[c_1] \geq 0.35$ are 29512-013 and 30312-062, which have $[c_1] \sim 0.8$ and which were classified as "TO" by BPSII, and 22945-063, 22958-037, and 29501-051, which were classified "SG" and which have $0.376 \leq [c_1] \leq 0.514$. The first two were obviously mis-classified by BPSII. All five lacked UBV photometry in the BPSII catalogue, and since the BPSII classification scheme involved the stars' positions in the dereddened two-color diagram, $(U-B)_0$ versus $(B-V)_0$, stars without complete photometric data could be easily mis-classified. As BPSII admit, "For the stars which lack photometry, we are forced to assign the blue stars types TO (thus mistyping a number of FHB stars), and the red-star types of G (thus mistyping a number of AGB stars)."

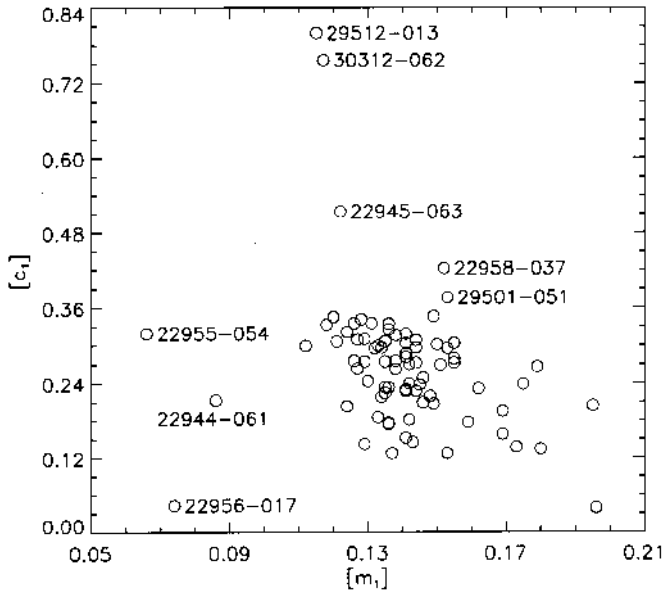

Fig. 5. The $[c_1]$, $[m_1]$ diagram for the 80 southern BPSII stars with spectroscopic $[Fe/H]_c$ values; all stars have $[Fe/H]_c \leq -2.5$

In Fig. 5 three stars are seen with $[m_1] \lesssim 0.094$: 22944-061, 22955-054, and 22956-017; these are much bluer in $[m_1]$ than the majority of stars. The latter two of these do not have UBV data in the BPSII catalogue but do have $(B-V)$ values of 0.41 and 0.40, respectively, estimated from the Balmer-line HP index. However, 22955-054 and 22956-017 have in Table 1 $(b-y)$ values much bluer than the other BPSII stars. Perhaps they are mis-classified sdB stars. The third of these stars, 22944-061, has the most negative observed m_1 index of all the stars in Table 1.

In Fig. 5 eight stars are plotted with $[m_1] \gtrsim 0.17$, larger than might be expected for stars with $[Fe/H] \leq -2.5$. It will be shown below that the photometrically derived [Fe/H]'s for seven of these stars are considerably higher, by $3-5\sigma_{[Fe/H]}$, than the spectroscopic $[Fe/H]_c$'s, where $\sigma_{[Fe/H]}$ is the estimated standard deviation of the photometric values. These seven stars probably have some anomaly, such as an unusual chemical abundance ratio or a binary companion. Four of these stars were identified by BPSII as having "...unusually strong G bands and CN features." The eighth of these stars, 22877-013 with the largest $[m_1]$ and smallest $[c_1]$, falls outside the range of our intrinsic-color calibration, and so a reliable photometric [Fe/H] value could not be obtained.

In Fig. 6 is presented the c_0, $(b-y)_0$ diagram for the same 80 BPSII stars as in Fig. 5. For many of these stars the c_0 and $(b-y)_0$ values have been obtained by correcting for interstellar reddening using the intrinsic-color calibration of Paper II and the techniques discussed there. The photometry has been corrected for reddening only when $E(b-y) \geq 0.015$. Previously the limit $E(b-y) \geq 0.025$ had been used in the Papers of this series, but spectroscopic studies involving the interstellar Ca line have shown that stars with $0.015 \lesssim E(b-y) \lesssim 0.025$ are in fact slightly reddened by interstellar matter (Nissen 1994). Also, some of the stars of Fig. 6 lie outside the ranges of our intrinsic-color calibration; for example, they have $\beta < 2.55$, $m_1 < 0.00$, or $c_1 > 0.57$. For these no photometric reddening estimate could be made, and so c_0 and $(b-y)_0$ have been merely set equal to the observed values c_1 and $(b-y)$. Therefore, Fig. 6 is somewhat more affected by interstellar reddening than Fig. 5.

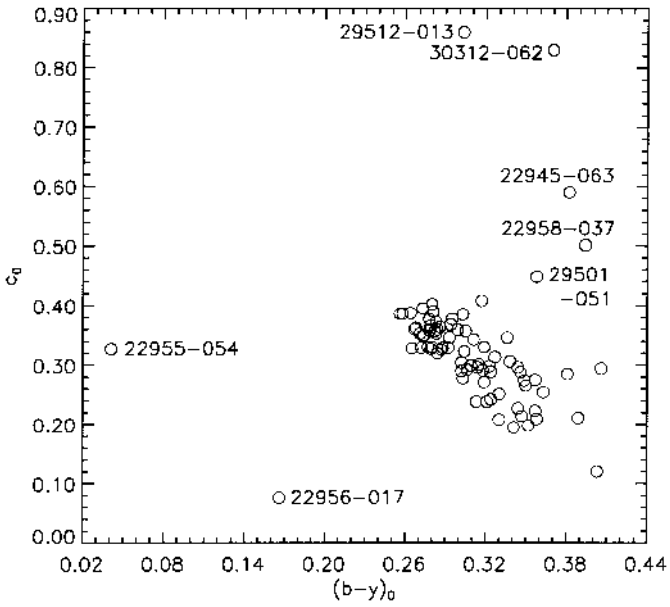

Fig. 6. The c_0, $(b-y)_0$ diagram for the same 80 BPSII stars as in Fig. 5

However, the c_0, $(b-y)_0$ diagram of Fig. 6 is similar to an HR diagram in that $(b-y)_0$ mostly measures temperature while c_0 is a gravity indicator. It can easily be compared to the c_0, $(b-y)_0$ diagrams for metal-poor stars found in Paper III. Figure 6 shows several of the same features as Fig. 5, a clump of MS and TO stars within the limits, $0.26 \lesssim (b-y)_0 \lesssim 0.36$ and $0.20 \lesssim c_0 \lesssim 0.40$, evolved stars for $c_0 \gtrsim 0.45$, and two blue sub-MS stars with $(b-y)_0 < 0.18$. A comparison between Fig. 6 and the c_0, $(b-y)_0$ diagrams of Paper III (especially Figs. 1 and 2) would indicate that probably the three stars with $0.45 \lesssim c_0 \lesssim 0.60$, 22945-063, 22958-037, and 29501-051, are in fact horizontal branch stars and that the two with $c_0 > 0.80$, 29512-013 and 30312-062, probably metal-poor supergiants; detailed spectroscopic observations are needed for confirmation. It is interesting to note that BPSII do not give values for the GP (G band) index for 29512-013 and 30312-062; this indicates that the measured index was consistent with a zero value. Also, as mentioned above in Sect. 2.4, the star 29512-013 has shown strong evidence of photometric variability.

Two stars, 22186-002 and 22944-061, with $c_0 \approx 0.30$ and $0.38 \lesssim (b-y)_0 \lesssim 0.41$ may be evolving along the metal-poor subgiant sequence detected in Paper III, Figs. 1–3. However, in Fig. 5, 22944-061 is the third star with $[m_1] \lesssim 0.09$, appearing more like a blue subluminous star.

The stars of Figs. 5 and 6 have also been plotted in the reddening-free $[c_1]$, β diagram, Fig. 7, also suggested by Strömgren (1966) for the study of F-type stars. This diagram too is similar to an HR diagram with β measuring $T_{\rm eff}$, and $[c_1]$ the stars' luminosities or surface gravities. The main features of Fig. 7 are similar to those of Figs. 5 and 6; most MS and TO stars lie in a band with $0.12 \lesssim [c_1] \lesssim 0.35$, and the evolved stars have $[c_1] \gtrsim 0.35$, but several details are different. The star 22186-002 is seen to lie above other stars in this figure with comparable β values and so remains a good candidate for being a metal-poor subgiant; 22944-061 is not so clearly separated from the other stars, and so its classification remains doubtful. In Figs. 6 and 7 the star 22171-037 stands somewhat above and to the right of the main clump of MS and TO stars and so also becomes a candidate for being a horizontal branch or giant star. And finally, the star 22955-054 appears in Figs. 5 and 6 like a blue, sub-MS star, but in Fig. 7 its position is more that of a blue straggler, with $\beta = 2.659$ and $[c_1] = 0.319$.

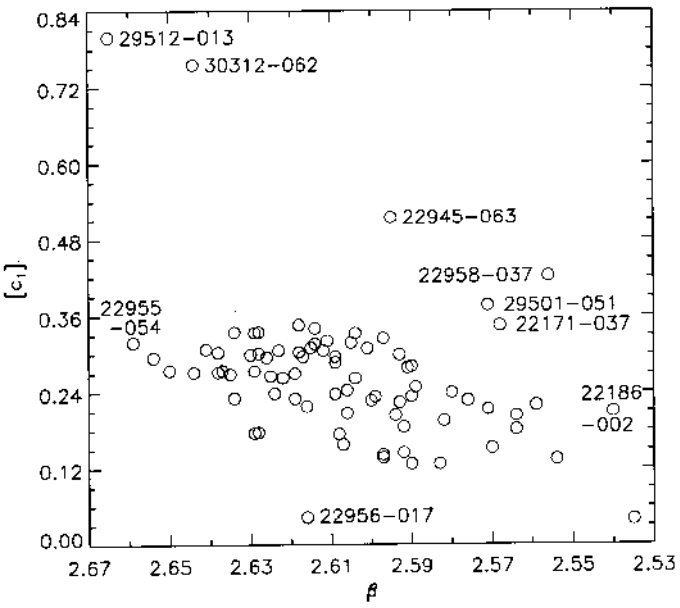

Fig. 7. The $[c_1]$, β diagram for the same stars as Figs. 5 and 6

About 90% of the "TO" stars have been classified correctly by BPSII according to our *uvby-β* photometry. However, of the 14 "SG" stars from BPSII plotted in Figs. 5–7, not one appears unambiguously to be a metal-poor subgiant; three are most likely horizontal branch stars, and eleven appear as MS stars. These errors are due in part to the lack of UBV photometry for five of the "SG" candidates and in part to the interstellar reddening offset to be discussed below; had BPSII used the reddening values from our intrinsic-color calibration, ten of the "SG" stars would have been classified instead "TO" stars.

3.2. *Stellar parameters from the uvby-β photometry*

As a prelude to the further analyses in this paper and to future spectroscopic studies, stellar parameters, such as $E(b-y)$, [Fe/H], M_V, δM_V, and $T_{\rm eff}$, are derived and discussed here. Several caveats are in order. First, for $[{\rm Fe/H}] \lesssim -2.0$ the metallicity index m_1 has lost most of its sensitivity to metallicity, and so in general the spectroscopic values of $[{\rm Fe/H}]_{\rm c}$ from BPSII, based on the CaII K absorption line, are more accurate and will be substituted whenever possible for the photometric [Fe/H] values. Second, our photometric [Fe/H] calibration (Paper II) was based on older high-resolution spectroscopic values from the literature. In Paper II it was shown that this photometric [Fe/H] calibration gives metallicities that are too high for stars with $[{\rm Fe/H}] \lesssim -1.0$ when compared to those from more modern high-resolution spectroscopy. In Paper II (Fig. 5) a conversion factor of 1.15 was obtained; in the following analyses our photometric [Fe/H] values will be multiplied by 1.15 when comparing with the BPSII values (or their values divided by 1.15). Third, most of the photometric calibrations to be used, such as those of Paper II, Paper V, and Magain (1987), have been obtained using calibration stars less metal-poor than many of the program stars of this paper. For example, the intrinsic-color calibration of Paper II included stars with metallicities only as low as $[{\rm Fe/H}] = -2.49$; the F-star [Fe/H] calibration as low as -3.5. So, the use of these calibrations then implies some small extrapolation outside the range of their intended use. This problem is mitigated somewhat by the conversion factor for the [Fe/H] values mentioned above.

In Table 2 are presented the stellar parameters $E(b-y)$, $[{\rm Fe/H}]_{\rm phot}$, M_V, δM_V and $T_{\rm eff}$ for all stars except the one (22960-029) that was misidentified. These parameters come from the calibrations of Papers II and V, and for $T_{\rm eff}$ from the calibration of Magain (1987). Only 69 stars have complete data in Table 2 since 16 BPSII stars fall outside the applicable photometric ranges of our photometric calibrations. In Table 2 Col. 1 gives the stellar designations according to BPSII; Cols. 2 and 3, the values of $E(b-y)$ and its estimated error, $\sigma_{E(b-y)}$, respectively; Cols. 4–6, the BPSII value of $[{\rm Fe/H}]_{\rm c}$, the photometric metallicity, $[{\rm Fe/H}]_{\rm phot}$, and the estimated error of $[{\rm Fe/H}]_{\rm phot}$, respectively; Cols. 7–8, the photometric absolute visual magnitude, M_V, and its estimated error; Cols. 9–10, the evolutionary correction δM_V, as defined in Paper V, and its estimated error; and Cols. 11–12, the value of $T_{\rm eff}$ from Magain's 1987 empirical calibration, and its estimated error. The spectroscopic metallicities have been used in the derivation of the last six columns. The estimated errors

have been derived by perturbing the input values of $(b-y)$, m_1, and c_1 by $\pm 0\overset{\mathrm{m}}{.}002$ and the input [Fe/H] by ± 0.10, and then scaling the output perturbations in the stellar parameters according to the observational errors given in the graphs of Fig. 1; $\sigma_{[\mathrm{Fe/H}]}$ for the BPSII values has been assumed to be ± 0.20. The scaled output perturbations have then been combined quadratically to give the final estimated standard deviations of Table 2. The quadratic combination of the errors assumes that they are independent, which is not strictly the case for the errors of the photometric indices $(b-y)$, m_1, and c_1.

These estimated errors will have relevance in several future studies. The T_{eff}'s will be part of the input into the model-atmosphere analysis of high-resolution spectroscopy; the $\log g$ input will follow from stellar classifications, such as from Figs. 5–7. The errors of M_V will propagate into the distance determinations necessary for kinematic analyses of the BPSII stars. And, within this paper the δM_V, $\log T_{\mathrm{eff}}$ plane will be compared to theoretical isochrones for age determinations. One can see in Table 2 that a typical error for $E(b-y)$ is about 0.014, for M_V about 0.25, for δM_V about 0.33, and for T_{eff} about 85 K. The estimated errors for $[\mathrm{Fe/H}]_{\mathrm{phot}}$ depend rather strongly upon its value; the errors grow quickly for $[\mathrm{Fe/H}]_{\mathrm{phot}} < -2.5$ due to the decreased sensitivity of m_1 to metallicity. The median estimated error for $[\mathrm{Fe/H}]_{\mathrm{phot}}$ in Table 2 is 0.64; the average estimated error for $[\mathrm{Fe/H}]_{\mathrm{phot}} > -3.0$ is 0.59.

3.2.1. Interstellar reddening

In addition to the color excess, $E(b-y)$, derived from the *uvby-β* photometry, we have obtained $E(B-V)$ by an automatic implementation of the Burstein & Heiles (1982) maps of the interstellar reddening derived from H I column densities as a function of Galactic longitude and latitude. Since this method of determining $E(B-V)$ is frequently used and is claimed to estimate $E(B-V)$ with an accuracy of ± 0.01, it is interesting to make a comparison with the $E(b-y)$ values given in Table 2.

As seen in Table 2 some stars have rather large errors of $E(b-y)$, $\gtrsim 0.02$, due either to relatively few observations of β or to a value in the range $2.55 < \beta < 2.58$, where β is less sensitive to temperature. In the comparison with $E(B-V)$, stars with $\sigma_{E(b-y)} \geq 0.020$ have been omitted. For the large majority of the remaining 66 stars the errors of $E(b-y)$ are between 0.010 and 0.015.

Figure 8 shows $E(B-V)$ plotted against $E(b-y)$ for this restricted sample. For comparison the expected relation, $E(B-V) = 1.35E(b-y)$, (Crawford 1975a) is shown. A significant offset from this line amounting to $\Delta E(b-y) \simeq 0.03$ is seen. Apart from this zero-point difference the scatter in the diagram is satisfactorily small. The discrepancy in the zero-point accentuates a long standing discussion about the interstellar extinction towards the Galactic Poles; see Burstein & Heiles (1982). 22 stars in Table 2 are situated in the South Galactic Pole (SGP) region, here defined by $b < -60°$. They have distances ranging from 0.3 to 1.8 Kpc. The average reddening of these stars is $E(b-y) = 0.027 \pm 0.004$ corresponding to $E(B-V) = 0.036 \pm 0.005$ significantly higher than the value, $E(B-V) = 0.008 \pm 0.002$, derived from the Burstein & Heiles maps for the same 22 stars. Furthermore, it should be noted that the reddening is not uniform; $E(b-y)$ ranges from zero to about 0.05. Burstein & Heiles (1982) claim that earlier studies of reddening at the Galactic Poles based on *uvby-β* photometry have given contradictory results. Knude (1977) derived an average reddening of $E(b-y) = 0.033$ for 73 A and F stars with $d > 100$ pc in 11 selected areas with $b < -50°$, whereas Kilkenny (1980) obtained $E(b-y) = 0.022$ for 29 B stars with $z > 500$ pc and $b < -45°$. In view of the rather small samples of stars studied and the patchy distribution of the reddening in the SGP region, both values are in fact in excellent agreement with our average value of $E(b-y) = 0.027$.

Independent evidence for a zero-point error in the Burstein & Heiles maps at the SGP comes from Geneva photometry and polarimetry. Nicolet (1982), derived an average value of $E(B-V) = 0.04$ for 15 B and A stars with $b < -60°$ and Appenzeller (1975) obtained a lower limit, $E(B-V) > 0.016$, from polarization data for 28 stars with $d > 100$ pc and $b < -70°$.

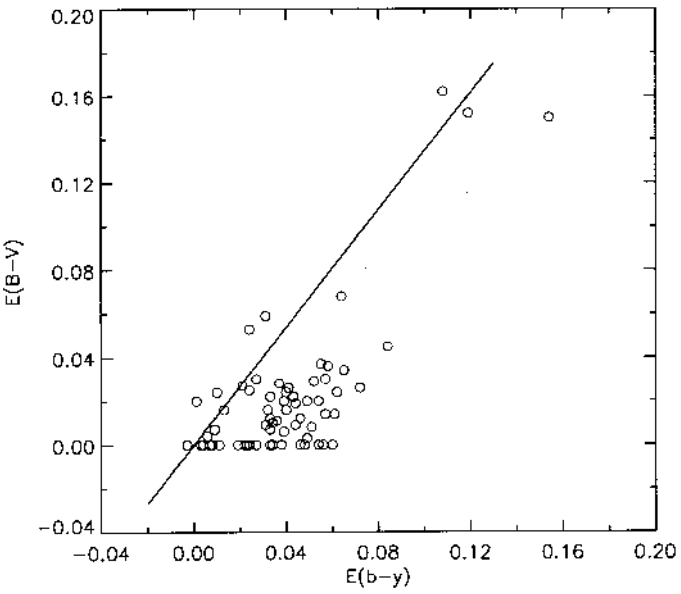

Fig. 8. The color excess $E(B-V)$ derived from the reddening maps of Burstein & Heiles (1982) versus $E(b-y)$. The expected relation, $E(B-V) = 1.35\,E(b-y)$, is drawn

Preston et al. (1991) obtained interstellar reddening estimates for a number of their fields based on a comparison of the observed distribution of colors for field horizontal-branch stars with that obtained for such stars at

Galactic latitudes $|b| > 55°$. Invoking the assumption that the high latitude fields (near the SGP) were essentially reddening free, they were able to produce estimates of color excess which are in substantial agreement with those obtained from the Burstein & Heiles maps (the possible exception being in the direction toward the Galactic bulge). Thus, the reported differences in reddening between claims based on *uvby-β* photometry and those obtained from the Burstein & Heiles maps would appear to be in the nature of a zero-point offset, rather than some increased dispersion in one or the other method.

It should be noted that the discussion of reddening differences amounting to $\Delta E(b-y) \simeq 0.03$ is of more than academic interest. With our $E(b-y)$ values the effective temperatures of the VMP stars derived from $(b-y)$ or $(B-V)$ become about 200 K higher than those derived with the Burstein & Heiles zero point — highly significant in connection with studies of the chemical compositions and the ages of these stars.

3.2.2. The [Fe/H] values

In Table 2 are seen seven stars for which the values of $[\mathrm{Fe/H}]_\mathrm{c}$ from BPSII, scaled by 1.15, and our photometric values, $[\mathrm{Fe/H}]_\mathrm{phot}$ differ by more than 3.5 times the estimated photometric error in Col. 6. These seven stars are also amongst the eight stars in Fig. 5 with the largest $[m_1]$ values. These seven stars are: 22169-008, 22881-036, 22898-027, 22898-047, 22949-008, 22958-042, and 29493-062. Four of these stars, 22881-036, 22898-027, 22949-008, and 22958-042 have been identified by BPSII as having, "...unusually strong G bands and CN features" according to their GP indices. It appears that the composition anomalies of these stars have affected the m_1 and c_1 indices of the Strömgren photometry leading to systematic errors in the $[\mathrm{Fe/H}]_\mathrm{phot}$ determinations, but other explanations (such as binary-star contamination or measurement errors) may be required for the remaining stars. The star 22877-013 is too red for an $[\mathrm{Fe/H}]_\mathrm{phot}$ determination, but it also falls in the category of having some sort of photometric and/or spectroscopic anomaly; its $[m_1]$ is much too large for its $[\mathrm{Fe/H}]_\mathrm{c}$ value.

3.2.3. Distances and absolute magnitudes

In Fig. 9 is shown a comparison of the stellar distances from BPSII with those from our photometric calibrations as described in Paper V. As shown above our visual magnitudes agree very well with those of BPSII, and so the differences of Fig. 9 reflect mainly the differences between our absolute visual magnitude calibrations, as well as differing classifications for the BPSII stars. Our method includes an evolutionary correction of the form, $\delta M_V = f\delta c_0$, and so accurate values for M_V should be obtained even for subgiant and evolving MS stars. δc_0 is determined using empirical calibrations, and the f coefficient is from the work of Nissen et al. (1987). The zero-point of our M_V calibration is based upon the mean relations of Crawford (1975b) and of Olsen (1984), and the displacement of the ZAMS in the M_V, $(b-y)_0$ diagram as a function of metallicity, upon the stellar models of VB85. In Fig. 1 of Paper V our M_V values have been compared to those from trigonometric parallaxes for the stars from the SN catalogue. No systematic difference larger than about $0\overset{\mathrm{m}}{.}2$ was found for the 14 stars with $[\mathrm{Fe/H}] < -1.0$. The M_V values of BPSII are based upon the Revised Yale Isochrones (Green et al. 1987); their calibration procedure is described by Beers et al. (1990).

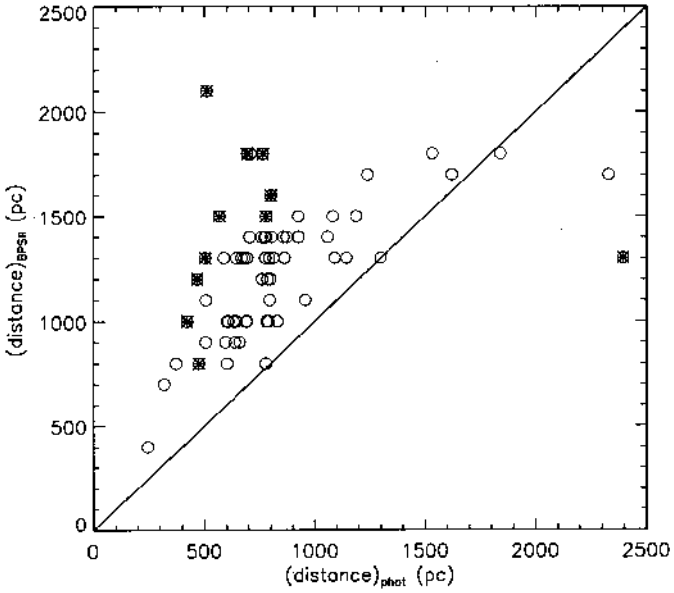

Fig. 9. A comparison of the stellar distances from BPSII with those from the *uvby-β* photometry. Open circles represent the "TO" stars of BPSII while the starred circles "SG" stars. The diagonal line shows the one-to-one relation

In Fig. 9 subgiant stars according to BPSII are indicated by starred circles, "TO" stars by open circles, and the points at right with *uvby-β* distances of 2395 and 2329 pc and BPSII distances of 1300 and 1700 pc correspond to the stars 29501-051 and 22171-037, respectively, which are horizontal branch stars according to the discussion of Sect. 3.1. Two things are obvious from Fig. 9. First, the BPSII distances are mostly larger than the *uvby-β* values, and second, the largest discrepancies (by factors as large as three) occur for the stars classified as "SG" by BPSII. This agrees with the conclusions of Sect. 3.1 (Figs. 5–7), that all of the supposed subgiant stars in our sample ("SG" types from BPSII) have been mis-classified; one (29501-051) is a horizontal branch star, and the rest are MS stars.

But even for the TO types, which *have* been classified correctly, there is still a significant systematic difference in Fig. 9. Part of this is due to the way that BPSII assign M_V values to the TO stars; for each TO star they take an

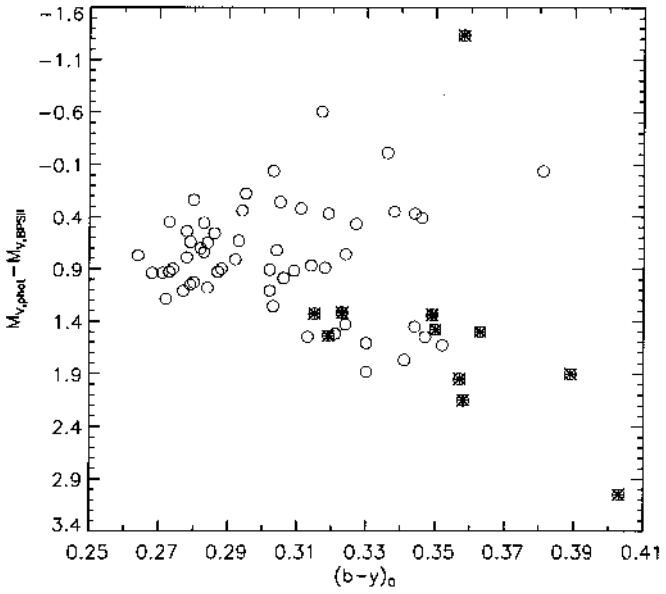

Fig. 10. The differences between the absolute visual magnitudes derived from the *uvby-β* photometry and those from BPSII have been plotted against the stars' $(b-y)_0$ values. Open circles represent the "TO" stars of BPSII while the starred circles "SG" stars

average of the two possible M_V values the star might have on the Revised Yale Isochrones according to its $(B-V)$ value, one M_V value from the evolving MS below the turn-off and one from the branch above the turn-off. In fact many TO stars will lie along the evolving MS below the turn-off point and will have fainter M_V's as can be seen in Fig. 2 of Beers et al. (1990); only a very few will have brighter M_V's than those assigned, due to the shape of the isochrones. This effect explains part of the scatter to the left of the one-to-one line in Fig. 9 for the TO stars. But, a plot of $(M_{V,\rm phot}-M_{V,\rm BPSII})$ versus $(b-y)_0$, Fig. 10, indicates that even for the bluest TO stars there is still a systematic difference of $0\overset{\rm m}{.}7-1\overset{\rm m}{.}0$, with the $M_{V,\rm phot}$ values being the larger. In Fig. 10 only a few of the redder more evolved stars have ΔM_V values near zero, and many of the less-evolved TO stars and all but one of the SG stars have differences greater than $+1\overset{\rm m}{.}0$. These systematic differences are due in part to the mis-classifications and also to the different calibration procedures used, to the different isochrones and stellar models employed, and in some cases to the extrapolations to lower metallicities required. Such systematic differences would indicate that the photometric and spectroscopic distances of such VMP stars are probably much less accurate than the errors usually quoted for metal-poor stars and point out the need for good stellar models and isochrones to even lower metallicities than usually computed.

3.3. *The* $(b-y)_0$,*[Fe/H] diagram*

In Fig. 11 is given the $(b-y)_0$,[Fe/H] diagram for three groups of stars. The first group is the same set of 80 BPSII stars that has been analyzed in Figs. 5–7. The [Fe/H] values plotted for these stars are the $[{\rm Fe/H}]_{\rm c}$ spectroscopic ones from BPSII. The second group is the sample of 280 "halo" stars that have been studied in the kinematic and metallicity analyses of the SPC catalogue and in the age analyses of Paper VII. These halo stars were separated from the thin- and thick-disk stellar populations using a diagonal cut in the $V_{\rm rot}$, [Fe/H] diagram and are thought to comprise a nearly pure halo sample, with less than six contaminating thick-disk stars. The photometric [Fe/H] values for these halo stars have been scaled by the factor 1.15, as discussed above. The third stellar group of Fig. 11 is a somewhat more contaminated "thick-disk" sample of 275 stars. In SPC a thick-disk sample of 74 stars was selected using two diagonal cuts in the $V_{\rm rot}$, [Fe/H] diagram, $-12 \le X \le -18$, where X is a linear combination of $V_{\rm rot}$ and [Fe/H]. This thick-disk sample was thought to be fairly pure with only 2–3 contaminating thin-disk stars and 2–3 contaminating halo stars; these estimates for the contamination came from the Gaussian fitting of our mixture-model analyses. (The above halo sample is the set of 280 stars with $X > 0.0$). For the "thick-disk" sample of Fig. 11 the selection criteria have been widened, $-12 \le X \le -5$, to obtain a larger sample but at the risk of allowing in more contaminating halo stars. Our mixture-model analyses would still estimate 2–3 contaminating thin-disk stars in the "thick-disk" sample of Fig. 11 but now roughly 30–35 contaminating halo stars.

Also plotted in Fig. 11 are the turn-off loci of the 8, 15, and 18 Gyr isochrones from BV92; that is, the blue-most points of the isochrones are plotted as a function of [Fe/H]. Since the most metal-poor isochrones of BV92 are those for [Fe/H]$= -2.26$, the more metal-poor parts of these curves have been extrapolated using polynomials fit to the isochrones in the δM_V, $\log T_{\rm eff}$ plane. So, in Fig. 11 the isochrone curves are less accurate for $[{\rm Fe/H}] \lesssim -2.3$ due to this extrapolation. The conversion from $T_{\rm eff}$ to $(b-y)_0$ has been made using the calibration of Magain (1987), which includes a term that takes into account [Fe/H] differences.

The bluest MS stars of each stellar population should be from the youngest component of that population, and, depending on completeness and observational errors, at or near the turn-off color corresponding to that component's age. It can be concluded from Fig. 11 that the youngest stars from the BPSII and halo groups are coeval to within 1−2 Gyr, with ages somewhat larger than 18 Gyr on the BV92 system of ages. (It was seen in Paper VII that the VB85, V85, and BV92 isochrones, when used with the techniques described below, give ages with systematic offsets). If any age difference can be inferred from Fig. 11, it is in the sense that the BPSII stars may be slightly younger than the halo stars, which are mostly stars within

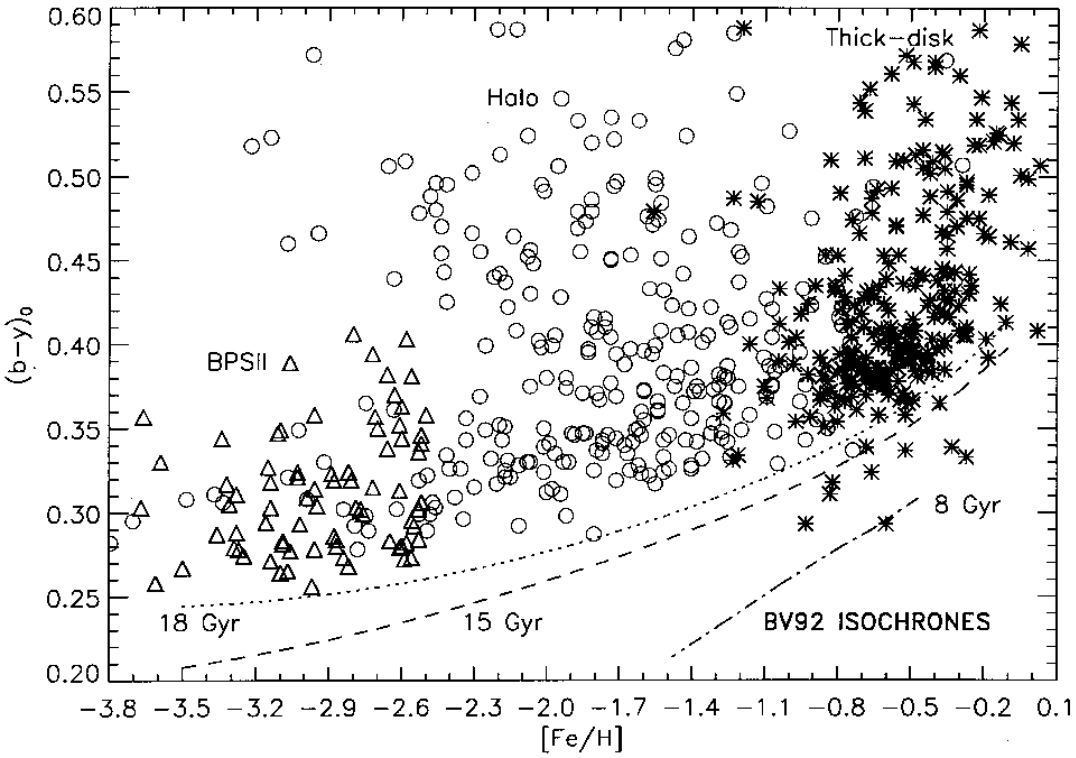

Fig. 11. The $(b-y)_0$, [Fe/H] diagram for the BPSII stars, and for halo and "thick-disk" stars from the SN and SPC catalogues, as described in the text. The metallicities for the BPSII stars are the spectroscopic ones from the HK survey, while scaled photometric values from the *uvby-β* data have been used for the halo stars. Also drawn are the turn-off loci for the 8, 15, and 18 Gyr isochrones of BV92. Conversion from $T_{\rm eff}$ to $(b-y)_0$ has been made using the calibration of Magain (1987)

300 pc of the Sun. In Paper VII an average age for 44 of the halo stars was obtained, $\langle Age\rangle \simeq 20$ Gyr, on the BV92 system using the unscaled photometric [Fe/H] values. This is somewhat larger than might be inferred from Fig. 11, but this figure gives no information upon the range of ages within a given stellar group; older evolving stars, which correspond to redder turn-offs, are not distinguishable in Fig. 11. In Papers III and VII it has been argued that there is a range of age of 3−5 Gyr in the halo field stars; evolving halo stars at a given [Fe/H] were found over a significant range in $(b-y)_0$ and in $\log T_{\rm eff}$. The results of Preston et al. (1994; PBS) would indicate perhaps an even larger range in ages for the halo.

Due to the selection criteria of BPSII, mainly the criterion HP < 4.0, good examples should not be found in our sample for the "blue metal-poor main sequence stars" (BMP stars) that have been detected by PBS. These are stars with [Fe/H]≤ -1.0 that fall blueward of the globular cluster MS turn-offs in the $(U-B)_0, (B-V)_0$ color-color diagram. They argue that these are stars accreted by the Galaxy during the last 3 to 10 Gyr, probably from dwarf spheroidal galaxies. In fact, three of the stars from our Table 1, 22171-037, 22873-139, and 22964-214, are also found in Table 1 of PBS, which gives BMP stars identified using the UBV photometry from their HK survey. These three stars do not appear especially blue in Fig. 11 as function of their $[{\rm Fe/H}]_{\rm c}$ values; they have $([{\rm Fe/H}],\ (b-y)_0) = (-3.32, 0.317)$, $(-3.14, 0.271)$, and $(-3.29, 0.279)$, respectively. All three lie well above the 18 Gyr curve. As expected, these three stars are not really the best examples of BMP's. They have $(B-V)_0$ values of 0.343, 0.344, and 0.335, respectively, and so lie very close to the nearly vertical blanketing vector in the $(U-B)_0, (B-V)_0$ diagram used by PBS to separate the BMP's from the globular-cluster-like turn-off stars.

The star 22873-139 is now a known double-lined spectroscopic binary star, as discussed in detail by Preston (1994). In fact, Preston shows that the inferred colors of the *primary* star of this binary are solidly into the BMP region with $(B-V)_0 = 0.30$ and $(U-B)_0 = -0.19$. The derived mass and luminosity ratios of the components of this binary imply an age on the order of 8 Gyr for [Fe/H]$= -3.1$.

However, Fig. 11 does perhaps show some evidence for BMP's in the less metal-poor "thick-disk" group. A large clump of thick-disk stars is seen to lie just above the 18 Gyr curve in Fig. 11 indicating that, as has been argued in Papers III and VII, the thick-disk is coeval to within 1−2 Gyr with the halo. The large majority of "thick-disk" stars are seen to come from a population that is as old or older

than 18 Gyr on the BV92 system. But, in Fig. 11 eleven stars are seen to lie on or below the 15 Gyr curve. (Five of these are also found in the cleaner thick-disk sample of 74 stars discussed in SPC and in Paper VII.) From the mixture-model fitting of SPC, it can be argued that 2–3 of these stars are probably contaminating thin-disk stars. From the selection criterion used to define this "thick-disk" sample, $-21 \leq X \leq -5$, it could be expected that most contamination comes from the halo population, but in Fig. 11 the adjacent halo group shows only one star on or below the 18 Gyr curve. This star W7547 has been discussed in SPC as having very uncertain kinematics due to a very uncertain proper motion; it may in fact not be a halo star. So, it is not probable that all of the bluer thick-disk stars of Fig. 11 can be attributed to contamination by halo stars like those of the solar neighborhood.

A more detailed look at the kinematics of the eleven stars mentioned above shows four to have old thin-disk-like velocity components, $|U'| < 60$ km s^{-1}, $|V'| < 60$ km s^{-1}, and $|W'| < 40.0$ km s^{-1}; three of these are from the smaller, cleaner thick-disk sample of SPC and Paper VII. Two of the eleven have legitimate thick-disk kinematics with U''s of -64.8 and -57.9 km s^{-1}, V''s of -57.3 and -50.5 km s^{-1}, and W''s of -47.6 and -46.0 km s^{-1}. These two stars, HD 61902 and HD 106516, with $([\mathrm{Fe/H}], (b-y)_0) = (-0.66, 0.324)$ and $(-0.82, 0.318)$, respectively, are perhaps thick-disk equivalents to blue stragglers. The most interesting are the remaining five blue "thick-disk" stars from Fig. 11. These have $-0.93 \leq [\mathrm{Fe/H}]_{\mathrm{phot}} \leq -0.17$, but each one has at least one velocity component extreme for a thick-disk star, indicating a low rotation velocity about the Galaxy, $V_{\mathrm{rot}} < 140$ km s^{-1}, and/or a high velocity perpendicular to the Galactic plane, $|W'| > 80$ km s^{-1}, very similar to the BMP's of PBS. A sample of five stars is really too small to define well velocity dispersions, but these five give, $\langle V_{\mathrm{rot}} \rangle = 146.6$ km s^{-1}, $\sigma_U = 80$ km s^{-1}, $\sigma_V = 61$ km s^{-1}, and $\sigma_W = 141$ km s^{-1}. The BMP's of PBS gave, $\langle V_{\mathrm{rot}} \rangle = 128$ km s^{-1}, and $\sigma_U \cong \sigma_V \cong \sigma_W \cong 90$ km s^{-1}; more recent work with a larger sample has given (Wilhelm 1995), $\langle V_{\mathrm{rot}} \rangle = 117 \pm 21$ km s^{-1}, $\sigma_U = 71$ km s^{-1}, $\sigma_V = 109$ km s^{-1}, and $\sigma_W = 82$ km s^{-1}. It is not certain whether these bluer "thick-disk" stars of Fig. 11 are really thick-disk or contaminating halo, but their blue colors, ages as young as 7−8 Gyr (from the isochrones of BV92), and unusual kinematics intermediate between thick-disk and halo would indicate some connection to the BMP stars.

In Papers V and VII a scenario proposed by Freeman (1987, 1990) for the formation of the thick disk was discussed; it is based upon the ideas of Searle & Zinn (1978) concerning the accretion of intergalactic fragments for the formation of part of the Galactic halo. According to this scenario, the thick disk was formed by the dynamic heating of a primeval thin disk during this accretion of the halo, mostly the outer halo. In fact, in Paper VII evidence was found that not only is the thick disk as old as the halo to within 1−2 Gyr, but also that the thick-disk age is most similar to that of the outer halo. So then, perhaps the "thick-disk" stars of Fig. 11 give evidence confirming both the ideas of Paper VII and those of PBS, that most of the thick disk was formed some 18−20 Gyr ago (on the BV92 system) during the accretion of the Galactic halo, but that some accretion events á la PBS continued until as recently as 7−8 Gyr ago. The bluer "thick-disk" stars of Fig. 11 are from this more lengthy and more recent accretion process.

3.4. *Individual ages for the BPSII stars*

Ages have been determined for the individual BPSII stars making use of the same techniques described and utilized in Papers III, V, and VII. Briefly, the method of Paper III is an analytical one making use of coordinate transformations and polynomials fit in the c_0, $(b-y)_0$ diagram to the isochrones of VB85. The spectroscopic $[\mathrm{Fe/H}]_{\mathrm{c}}$ values have been used, divided by 1.15 to place them on the photometric [Fe/H] system of Paper II. The observational errors of the individual stars have been used to perturb the polynomials to give error estimates for the derived ages, σ_{Age}; only stars with $\sigma_{\mathrm{Age}} \leq 5.0$ Gyr have been retained for further discussion and analysis.

Seventeen such stars remain with a mean age and mean error of $\langle Age \rangle \pm \sigma = 20.8 \pm 0.9$ Gyr. In Paper VII, 70 halo stars had their ages estimated using the same method, giving mean values of 15.3 ± 0.4 Gyr. However, the halo sample from Paper VII was cleaned as much as possible of binary-star contamination. Removing the CH stars and the binary candidates from the BPSII sample, leaves 12 stars with the mean values of 19.9 ± 1.0 Gyr. This discrepancy between the results of Fig. 11 and the mean ages of the BPSII and halo stars may be related to the need to extrapolate the polynomials to the lower metallicities of the VMP BPSII stars.

The second method for determining stellar ages is the graphical one described in Papers V and VII, which makes use of the BV92 isochrones in the δM_V, $\log T_{\mathrm{eff}}$ plane. To maintain a reasonable precision, the ages have been measured only when a star has evolved sufficiently from its ZAMS, only when $\delta M_V > 0\overset{\mathrm{m}}{.}4$. For this method also the spectroscopic $[\mathrm{Fe/H}]_{\mathrm{c}}$ values have been converted to the photometric system by dividing by 1.15.

By this second method 28 BPSII stars with $\delta M_V > 0\overset{\mathrm{m}}{.}4$ have had their ages measured. The mean values are, $\langle Age \rangle \pm \sigma = 21.3 \pm 0.9$ Gyr on the BV92 system of ages. Removing the CH stars and possible binary stars leaves 24 stars with mean values of 20.6 ± 0.9 Gyr. In Paper VII the same method and same isochrones gave a mean age and error of 20.3 ± 0.5 Gyr for 44 halo stars. By this method there seems to be no significant discrepancy between that

which is seen in Fig. 11 and the mean ages from individual-star measures for the halo and BPSII groups.

In Papers III and VII it has been argued that there is a significant cosmological scatter in the ages of the halo field stars, with a real range of at least 3 Gyr. Such conclusions have been derived using the first method described above, that which makes use of polynomials fit to the VB85 isochrones. The observed scatter in the derived ages was compared to that expected from the observational errors in $(b-y)_0$, c_0, and $[\mathrm{Fe/H}]_{\mathrm{phot}}$. The observed scatter was larger than the expected by an amount that is significant at greater than a 99% confidence level. Such a result held in Paper VII even after the halo sample had been cleaned as much as possible of binary-star contamination. However, for these VMP stars the above analyses do not provide any significant evidence for such an age spread. Both the analytical method using the VB85 isochrones and the graphical method using BV92 indicate that the observed age spread is only slightly larger than that expected from the observational errors in $(b-y)_0$, c_0, and $[\mathrm{Fe/H}]_{\mathrm{c}}$. For the graphical method the errors of Table 2 have been used to estimate σ_{Age} for each of the BPSII stars. For these BPSII stars the detection of an age spread is more difficult due to their faintness and very low metallicities leading to generally larger estimated errors.

4. Conclusions

Our main conclusions are the following:

1) The *uvby-β* photometry for the 87 BPSII stars is of good quality. Mean observational errors for a star with $V = 14\overset{\mathrm{m}}{.}2$ have been estimated to be 0.008, 0.007, 0.011, 0.010 and 0.012 for V, $(b-y)$, m_1, c_1 and β, respectively.

2) Comparisons of V and $(b-y)$, from our *uvby-β* photometry, with V and $(B-V)$, respectively, from the HK survey, show reasonable agreement indicating that the two data sets are of good quality and that our error estimates are only slightly under-estimated. A comparison between β and the spectral index HP from the HK survey shows considerable scatter indicating that the estimated error of HP in BPSII is too low; $\sigma(\mathrm{HP}) = \pm 0.2$ Å is more realistic for the faint stars of this paper. Even so it is noted that the HP index gives as accurate a measure for T_{eff} as does β.

3) Using several of the reddening-free and reddening-corrected index diagrams of the *uvby-β* photometric system, it is found that several of the BPSII stars have been mis-classified. Not one of the fourteen "SG" stars are in fact found to be subgiants; three are more evolved, probably horizontal branch stars, and the other eleven are MS stars. In the sample are found two metal-poor supergiants, three or four horizontal branch stars, one blue subluminous star, one metal-poor subgiant like those identified in Paper III, and two stars with ambiguous classifications. BPSII have classified correctly about 90% of the "TO" stars.

4) Photometrically the stellar parameters, $E(b-y)$, [Fe/H] M_V, δM_V, T_{eff} and age have been measured for many of the 87 BPSII stars, and errors have been estimated for these parameters using a perturbation technique. Typical errors are about ± 0.014 for $E(b-y)$, ± 0.25 for M_V, ± 0.33 for δM_V, and ± 85 K for T_{eff} for these VMP stars. For $[\mathrm{Fe/H}] \leq -2.5$ the m_1 index has lost much of its sensitivity to metallicity, and so a typical error of ± 0.60 has been estimated for $[\mathrm{Fe/H}]_{\mathrm{phot}}$.

5) Our $E(b-y)$ values have been compared to the $E(B-V)$ values from the Burstein & Heiles (1982) maps. A systematic difference amounting to approximately $\Delta E(b-y) = 0.03$ has been found with our values being generally larger than would be expected from the maps.

6) Seven stars have been identified which have photometric metallicities, $[\mathrm{Fe/H}]_{\mathrm{phot}}$, larger than the scaled spectroscopic values, $[\mathrm{Fe/H}]_{\mathrm{c}}/1.15$, by more than 3.5 times the estimated error in $[\mathrm{Fe/H}]_{\mathrm{phot}}$. These stars are probably CH and/or binary stars.

7) In a comparison of the distances, a significant systematic difference is seen with the BPSII values being larger than our values by typically a factor of 1.5 and in some cases by a factor as large as three. This is due in part to the mis-classification by BPSII of some of the stars and also due to a systematic difference of about $0\overset{\mathrm{m}}{.}7-1\overset{\mathrm{m}}{.}0$ between our different calibration procedures. This points out two problems: systematic errors for such VMP stars can produce distance errors much larger than normally quoted for metal-poor stars, and stellar model calculations and empirical calibrations need to be extended now to these very low metallicities.

8) In the $(b-y)_0$,[Fe/H] diagram the youngest of the BPSII stars are seen to be coeval to within 1−2 Gyr with the youngest halo stars as defined previously, using a diagonal cut in the V_{rot},[Fe/H] diagram; if any age difference exists, it is in the sense that the BPSII stars are slightly younger than the local halo stars. And, the very large majority of "thick-disk" stars are also coeval with the other two stellar groups to within 1−2 Gyr. All three stellar groups appear to be slightly older than 18 Gyr on the BV92 system of ages.

9) A number of the "thick-disk" stars with $[\mathrm{Fe/H}] > -1.0$ have $(b-y)_0$ values bluer than the large majority of thick-disk stars, corresponding to ages as small as 7−8 Gyr on the BV92 system, and have unusual kinematics intermediate between halo and thick-disk. These stars are perhaps related to the "blue metal-poor main sequence stars" of PBS.

10) For both the BV92 and VB85 isochrones the observed scatter in the ages of the BPSII stars is only slightly larger than what would be expected from the observational errors in $(b-y)_0$, c_0, and $[\mathrm{Fe/H}]_{\mathrm{c}}$, and so unlike Papers III and VII, where a significant age spread was

Table 2. Stellar parameters for the 86 VMP stars. The columns are described in the text

STAR	$E(b-y)$	σ	$[Fe/H]_c$	$[Fe/H]_{phot}$	σ	M_V	σ	δM_V	σ	T_{eff}(K)	σ
16027−003	.034	.017	.....	−1.94	.32	4.07	.33	1.04	.51	6065	114
16027−073	.008	.020	.....	−1.53	.29	4.10	.27	1.42	.35	5747	63
16927−017	.048	.011	−3.20	−2.68	.37	4.40	.18	.90	.28	5963	73
16927−063	.006	.011	.....	−.58	.13	3.74	.22	1.00	.35	5991	56
22169−008	.010	.015	−2.88	−1.28	.33	4.09	.23	1.01	.30	6085	64
22171−037	−.029	.032	−3.32	−4.4:	....	3.10	.22	1.99	.30	6099	62
22174−020	.018	.028	−3.14	−2.68	1.36	3.67	.63	1.26	.88	6200	188
22177−009	.039	.011	−3.67	−2.85	.88	4.94	.17	.01	.24	6195	70
22177−010	.027	.013	−2.99	−2.23	.55	4.64	.25	.35	.36	6158	83
22180−014	.024	.009	−2.52	−2.75	.57	5.64	.15	−.31	.21	5932	52
22182−033	.034	.017	−2.66	−2.44	.62	4.14	.33	1.16	.49	5954	115
22186−002	.....	.....	−2.56	....	....	....	....	....	....	....	...
22186−017	.022	.012	−3.14	−2.27	.39	4.59	.19	.51	.31	6094	81
22872−102	.154	.009	−2.81	−2.07	.27	4.85	.14	.26	.22	6082	55
22873−072	.084	.015	−3.07	....	....	....	....	....	....	6465	93
22873−139	.049	.012	−3.14	−3.30	1.50	4.66	.25	−.05	.34	6423	76
22876−032	.003	.010	−4.37	−2.92	.44	5.29	.16	−.05	.17	6007	35
22877−013	.....	.....	−2.58	....	....	....	....	....	....	....	...
22877−051	.057	.015	−2.82	−2.45	1.02	4.73	.34	−.16	.45	6445	93
22878−027	.031	.010	−3.03	−1.77	.36	5.14	.13	.03	.18	6047	57
22879−012	.052	.021	−3.09	....	....	....	....	....	....	6352	139
22879−029	.033	.009	−2.52	−1.64	.31	4.85	.16	.10	.22	6175	54
22879−051	.044	.016	−2.84	−4.0:	....	4.24	.38	.38	.53	6409	110
22881−036	.007	.008	−2.96	−1.51	.18	5.19	.14	.34	.18	5810	41
22881−070	.060	.013	−2.97	....	....	....	....	....	....	6525	83
22884−033	.119	.014	−3.36	−2.00	.69	4.62	.22	.16	.33	6307	86
22884−108	.108	.009	−3.28	−1.85	.38	4.60	.16	.18	.23	6306	58
22888−014	.019	.012	−2.77	−2.40	.68	4.90	.22	.02	.30	6205	73
22888−031	.023	.013	−3.59	−3.26	1.48	5.56	.18	−.31	.24	6004	75
22890−011	.034	.018	−2.87	−2.08	.68	3.99	.43	.71	.59	6357	119
22892−025	.043	.010	−2.61	−2.36	.64	4.93	.19	−.26	.27	6367	63
22893−005	.072	.019	−2.60	−2.64	.79	4.50	.36	1.07	.53	5774	129
22893−015	.040	.016	−3.15	−2.20	.54	4.17	.28	1.03	.44	6027	107
22893−030	.061	.017	−2.89	−2.68	.71	4.44	.28	.72	.44	6054	108
22894−019	.040	.010	−3.03	−2.67	.62	5.23	.14	−.11	.21	6074	58
22894−049	.021	.015	−2.61	−2.04	.53	5.45	.25	.01	.35	5853	88
22898−027	.024	.008	−3.10	−1.12	.08	4.38	.14	1.05	.21	5871	51
22898−047	.058	.016	−3.06	−1.79	.16	4.80	.27	1.05	.41	5592	99
22942−024	.033	.011	−2.96	−1.84	.45	4.51	.22	.17	.30	6372	69
22943−095	.032	.009	−2.55	−2.38	.33	4.69	.20	.12	.28	6278	60
22943−132	.001	.012	−2.71	−2.64	.45	5.01	.13	.50	.16	5818	35
22944−014	−.027	.020	−2.52	−2.20	.42	4.29	.17	1.09	.22	5896	44
22944−061	.....	.....	−2.80	....	....	....	....	....	....	....	...
22945−017	.033	.011	−2.56	−1.95	.58	4.81	.21	−.20	.30	6408	71
22945−063	.....	.....	−2.66	....	....	....	....	....	....	....	...
22949−008	.037	.010	−2.72	−1.35	.23	4.55	.17	.49	.24	6116	62
22949−030	.024	.014	−2.96	−2.72	.65	4.59	.24	.46	.37	6123	92
22952−011	.052	.018	−3.16	−3.54	1.30	4.05	.37	.79	.55	6261	118
22953−037	.056	.011	−3.50	....	....	....	....	....	....	6448	73
22954−004	.046	.018	−2.76	....	....	....	....	....	....	6225	119
22955−054	.....	.....	−4.08	....	....	....	....	....	....	....	...
22956−017	.....	.....	−2.93	....	....	....	....	....	....	....	...
22957−019	.057	.011	−2.53	−3.68	1.61	4.95	.22	−.23	.32	6335	71
22957−024	.041	.015	−3.09	−2.96	1.13	4.45	.31	.28	.44	6340	97

Table 2. continued

STAR	$E(b-y)$	σ	$[Fe/H]_c$	$[Fe/H]_{phot}$	σ	M_V	σ	δM_V	σ	T_{eff}(K)	σ
22958−037	−.006	.047	−2.72	....	....	....	....	....	....	5557	62
22958−041	−.009	.033	−3.28	−2.39	.85	4.02	.25	1.00	.32	6141	65
22958−042	.004	.011	−3.34	−1.55	.30	5.14	.19	.25	.24	5909	56
22958−052	.031	.012	−2.87	−2.45	.56	4.39	.26	.35	.37	6329	81
22958−065	.000	.020	−2.60	−2.50	.72	4.19	.21	1.17	.27	5910	56
22958−074	.049	.011	−2.61	−2.70	.96	5.38	.17	−.36	.24	6128	67
22963−004	.096	.024	−3.66	....	....	....	....	....	....	5820	156
22964−214	.064	.012	−3.29	−3.60	1.26	4.34	.25	.35	.36	6369	81
22968−001	.003	.021	−2.82	−2.74	1.16	4.55	.25	.61	.33	6050	72
22968−026	.044	.013	−2.58	−2.05	.53	4.55	.28	.15	.39	6348	82
22968−029	.008	.011	−3.11	−2.42	.62	5.26	.18	.16	.22	5888	53
29493−050	.038	.012	−3.06	−2.77	1.06	4.82	.21	−.15	.30	6381	72
29493−062	.033	.011	−2.70	−1.58	.14	4.51	.21	.93	.31	5865	75
29493−094	.027	.016	−2.88	−2.87	.94	4.31	.33	.44	.48	6318	104
29499−003	.023	.021	−2.56	−2.41	.68	4.03	.50	.82	.72	6251	144
29499−060	.009	.013	−3.31	−2.29	.30	3.96	.13	1.01	.17	6183	35
29501−051	.071	.035	−2.50	−2.08	.43	1.81	.88	3.71	1.24	5808	244
29504−006	−.003	.016	−3.02	−2.45	.73	4.35	.21	.48	.28	6268	55
29506−007	.062	.014	−3.10	−3.17	1.79	4.48	.35	.07	.46	6472	94
29506−090	.054	.014	−3.25	−3.27	1.68	4.60	.25	.05	.37	6398	87
29512−013	.....	.....	−2.79	....	....	....	....	....	....	....	...
29512−015	.065	.016	−2.95	−2.59	1.00	4.43	.32	.52	.45	6189	100
29512−081	.055	.011	.....	−.89	.13	....	....	....	....	6386	73
29513−015	.046	.010	−2.59	−3.77	2.47	5.05	.18	−.44	.26	6413	61
29514−007	.051	.016	−3.27	−5.0:	....	4.24	3.78	.44	4.19	6375	109
29514−018	.039	.014	−2.65	−2.70	.62	4.32	.33	.40	.46	6336	95
29514−037	.036	.011	−2.60	−2.94	.98	4.89	.22	−.20	.31	6360	69
29527−015	.013	.017	−3.40	−3.49	1.19	3.75	.16	1.29	.21	6127	45
30312−062	.....	.....	−2.63	....	....	....	....	....	....	....	...
30339−069	.054	.017	−3.61	....	....	....	....	....	....	6512	108
30339−080	.027	.015	−2.53	−3.16	1.37	4.79	.31	.13	.44	6203	98
30493−071	.011	.016	−2.53	−1.91	.25	3.66	.15	1.62	.19	5966	36

found for the local halo stars, there is no significant evidence for such in these VMP stars.

Acknowledgements. We are indebted to T. Andersen for kindly loaning us his programs for reducing the *uvby-β* photometric data. This work was partially supported by grants from CONACyT (Mexico), Nos. D111–903865 and 1219–E9203, and DGAPA-UNAM project No. IN101495 and one of us (W.J.S.) is especially grateful to DGAPA, Subdirección de Formación Académica, de la Universidad Nacional Autonoma de México, for a sabbatical scholarship. We are very indebted to many of the technicians at SPM: specially to B. García, V. García, B. Hernandez, F. Lazo, E. López, J.M. Murillo, J.L. Ochoa and J. Valdez. T.C. Beers acknowledges support from NSF grant 92-22326. PEN acknowledges travel support from the Danish Board for Astronomical Research.

References

Appenzeller I., 1975, A&A 38, 313
Allen C., Schuster W.J., Poveda A., 1991, A&A 244, 280
Beers T.C., 1987, in: Nearly Normal Galaxies from the Planck Time to the Present. In: Faber S. (ed.). New York, Springer, p. 41
Beers T.C., Preston G.W., Shectman S.A., 1985, AJ 90, 2089 (BPSI)
Beers T.C., Preston G.W., Shectman S.A., Kage J.A., 1990, AJ 100, 849
Beers T.C., Preston G.W., Shectman S.A., 1992, AJ 103, 1987 (BPSII)
Beers T.C., Sommer-Larsen J., 1995, ApJS 96, 175
Bergbusch P.A., VandenBerg D.A., 1992, ApJS 81, 163 (BV92)
Boesgaard A.M., 1995, in: The Light Element Abundances, ESO Astrophysics Symposia. In: Crane P. (ed.). Springer-Verlag, p. 363
Burstein D., Heiles C., 1982, AJ 87, 1165
Carney B., 1993, in: Galaxy Evolution: The Milky Way Perspective. In: Majewski S.R. (ed.), ASP Conf. Ser. 49, p. 83
Crawford D.L., 1975a, PASP 87, 481

Crawford D.L., 1975b, AJ 80, 955
Crawford D.L., Barnes J.V., 1970, AJ 75, 978
Crawford D.L., Mander J., 1966, AJ 71, 114
Freeman K.C., 1987, ARA&A 25, 603
Freeman K.C., 1990, in: Astrophysics — Recent Progress and Future Possibilities, Invited Reviews at a Symposium in Honour of Bengt Strömgren. In: Gustafsson B. and Nissen P.E. (eds.), The Royal Danish Academy of Sciences and Letters, Mat. Fys. Medd. 42:4, p. 187
Green E.M., Demarque P., King C.R., 1987, The Revised Yale Isochrones and Luminosity Functions, Yale University Observatory, New Haven
Grønbech B., Olsen E.H., Strömgren B., 1976, A&AS 26, 155
Johnson H.L., Mitchell R.I., Iriarte B., Wisniewski W.Z., 1966, Commun. Lunar and Planetary Lab., No. 63, Univ. of Arizona, Tucson
Kilkenny D., 1980, MNRAS 191, 651
Knude J.K., 1977, Astrophys. Lett. 18, 115
Magain P., 1987, A&A 181, 323
Majewski S.R., 1992, ApJS 78, 87
Marquez A., Schuster W.J., 1994, A&AS 108, 341 (Paper VII)
McClure R.D., 1984, ApJ 280, L31
McWilliam A., Preston G.W., Sneden C., Searle L., 1995, AJ 109, 2757
Nicolet B., 1982, A&AS 47, 199
Nissen P.E., 1989, The Messenger 58, 40
Nissen P.E., 1994, in: Stars, Gas and Dust in the Galaxy, Invited Reviews at a Symposium in Honor of Eugenio E. Mendoza. In: Arellano Ferro A. and Rosado M. (eds.), Rev. Mex. Astr. Astrofis. 29, 129
Nissen P.E., Schuster W.J., 1991, A&A 251, 457 (Paper V)
Nissen P.E., Twarog B.A., Crawford D.L., 1987, AJ 93, 634
Norris J.E., Peterson R.C., Beers T.C., 1993, ApJ 415, 797
Olsen E.H., 1983, A&AS 54, 55
Olsen E.H., 1984, A&AS 57, 443
Press W.H., Teukolsky S.A., Vetterling W.T., Flannery B.P., 1992, Numerical Recipes in Fortran: The Art of Scientific Computing, Second Edition. Cambridge Univ. Press
Preston G.W., 1994, AJ 108, 2267
Preston G.W., Beers T.C., Shectman S.A., 1994, AJ 108, 538 (PBS)
Preston G.W., Shectman S.A., Beers T.C., 1991, ApJS 76, 1001
Schuster W.J., Nissen P.E., 1988, A&AS 73, 225 (SN)
Schuster W.J., Nissen P.E., 1989a, A&A 221, 65 (Paper II)
Schuster W.J., Nissen P.E., 1989b, A&A 222, 69 (Paper III)
Schuster W.J., Parrao L., Contreras Martínez M.E., 1993, A&AS 97, 951 (SPC)
Searle L., Zinn R., 1978, ApJ 225, 357
Strömgren B., 1966, ARA&A 4, 433
Thorburn J.A., 1994, ApJ 421, 318
Thorburn J.A., Beers T.C., 1992, BAAS 24, 1278
Thorburn J.A., Beers T.C., 1993, ApJ 404, L13
VandenBerg D.A., 1985, ApJS 58, 711 (V85)
VandenBerg D.A., Bell R.A., 1985, ApJS 58, 561 (VB85)
Vanture A.D., 1992, AJ 104, 1997
Wilhelm R., 1995, PhD Thesis, Michigan State University